

Magnetic moment suppression in Ba₃CoRu₂O₉: Hybridization effect

S. V. Streltsov*

*Institute of Metal Physics, S. Kovalevskoy Street 18, 620990 Ekaterinburg, Russia
and Institute of Physics and Technology, Ural Federal University, Mira Street 19, 620002 Ekaterinburg, Russia
(Received 23 April 2013; published 31 July 2013)*

An unusual orbital state was recently proposed to explain the magnetic and transport properties of Ba₃CoRu₂O₉ [H. Zhou *et al.*, *Phys. Rev. B* **85**, 041201 (2012)]. We show that this state contradicts the first Hund's rule and does not realize in the system under consideration because of a too small crystal-field splitting in the t_{2g} shell. A strong suppression of the local magnetic moment in Ba₃CoRu₂O₉ is attributed to a strong hybridization between the Ru 4*d* and O 2*p* states.

DOI: [10.1103/PhysRevB.88.024429](https://doi.org/10.1103/PhysRevB.88.024429)

PACS number(s): 75.25.-j, 75.30.Kz, 71.27.+a

I. INTRODUCTION

The 4*d*- and 5*d*-based transition-metal compounds have been widely investigated in the last few years. A larger spatial extension of the 4*d* and 5*d* wave functions and a substantial spin-orbit coupling makes them quite different from the 3*d* analogs in terms of the electronic and especially magnetic properties.

This, for instance, results in unusual zigzag antiferromagnetic order and a quasimolecular orbital state in Na₂IrO₃,¹ unconventional magnetic properties and a charge-ordered state sensitive to irradiation in Ba₃NaRu₂O₉,² formation of the spin singlets in La₄Ru₂O₁₀,³ and suppression of the magnetic moments in such compounds as Ba₄Ru₃O₁₀ (Ref. 4) and Ba₂NaOsO₆.⁵ A strong reduction of the local magnetic moment was also found in Ba₃CoRu₂O₉ (Refs. 6 and 7) and was recently attributed to a special type of the orbital order, which leads to an unusual orbital filling.⁸

Ba₃CoRu₂O₉ is a semiconductor⁹ and experiences a magnetic transition at $T_N = 93$ K, which is accompanied by the changes in the crystal symmetry from orthorhombic (*Cmcm*) in the low-temperature (LT) phase to hexagonal (*P6₃/mmc*) at higher temperatures.⁸ The Ru⁵⁺ ions are in the d^3 electronic configurations, while the Co ions show 2+ oxidation state with seven 3*d* electrons. Since the RuO₆ octahedra are strongly distorted,⁶ one may expect that the orbital moment is quenched and the total magnetic moment is defined by the spin component only. However, the neutron measurements show that the local magnetic moment on Ru in the LT phase is 1.17–1.45 μ_B according to Refs. 6 and 7, much smaller than 3 μ_B , which is expected for $S = 3/2$ from the naive atomic consideration. In contrast, the local magnetic moment on Co was found to be 2.71–2.75 μ_B ,^{6,9} which is close to the spin-only value of 3 μ_B for Co²⁺ ($S = 3/2$).

The reduction of the local magnetic moment on Ru⁵⁺ was explained in Ref. 8 as a result of the stabilization of an unconventional orbital state when one of the t_{2g} orbitals is completely filled (with spin-up and -down electrons), so that the total spin is $S = 1/2$ per Ru site (due to the remaining unpaired electron). This, however, contradicts the first Hund's rule, which states that the term with maximum spin (i.e., $S = 3/2$ in the case of the t_{2g}^3 configuration) has the lowest total energy. In a simple ionic model this “anti-Hund's rule” state is possible if the crystal-field splitting in the t_{2g} shell is larger than $2J_H$, which is quite unlikely since J_H is ~ 0.7 eV for Ru.¹⁰

In the present paper we investigate the electronic and magnetic structure of Ba₃CoRu₂O₉ using the band structure calculations and show that the splitting in the t_{2g} shell does not exceed 108 meV. As a result, the unconventional orbital state proposed in Ref. 8 is not realized. The suppression of the value of the local magnetic moment on Ru is explained by the hybridization effects with the O 2*p* states. Substantial hybridization between the Ru 4*d* and O 2*p* states leads to a localization of the electrons not on the atomic but on the Wannier orbitals, with a large contribution coming from the nonmagnetic O 2*p* states.

II. CALCULATION AND CRYSTAL STRUCTURE DETAILS

The linearized muffin-tin orbitals method (LMTO) was used in the calculations¹² with the von Barth–Hedin version of the exchange correlation potential.¹³ We investigated the effect of the possible strong Coulomb interaction on the *d* shells of the Ru and Co ions with the mean-field local spin-density approximation (LSDA) + *U* method.¹⁴ The on-site Coulomb repulsion parameter *U* and the intra-atomic Hund's rule exchange J_H were chosen as follows: $U(\text{Co}) = 6$ eV, $J_H(\text{Co}) = 1$ eV,¹⁵ $U(\text{Ru}) = 3$ eV, $J_H(\text{Ru}) = 0.7$ eV.¹⁰ In order to check the stability of the results these parameters were varied, as will be discussed. We used the mesh of the 144 *k* points in the full Brillouin zone in the course of the calculations.

The intersite exchange interaction parameters were calculated for the Heisenberg model written as

$$H = \sum_{ij} J \vec{S}_i \vec{S}_j \quad (1)$$

(i.e., each site is counted twice in the summation) using the Green's-function method described elsewhere.¹⁶

The crystal structure was taken from Ref. 6 for $T = 2$ K and is shown in Fig. 1. The Ru ions are placed in the center of the RuO₆ octahedra, which form dimers sharing their faces. These dimers are directed along the *c* axis, but the Ru-Ru dimer and the Ba-Ba pairs are alternating in the *c* direction. Three neighboring dimers lying in the same *ab* plane are interconnected by the CoO₆ octahedron. The CoO₆ and RuO₆ octahedra share one of the corners.

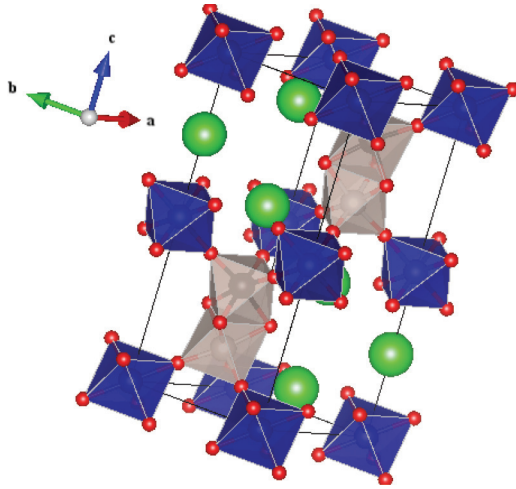


FIG. 1. (Color online) The crystal structure of $\text{Ba}_3\text{CoRu}_2\text{O}_9$. Oxygen ions are shown in red, and Ba ions are in green. Co^{2+} and Ru^{5+} ions are placed inside of the oxygen octahedra shaded blue and gray, respectively. The image was generated using VESTA software.¹¹

III. LOCAL-DENSITY APPROXIMATION RESULTS

We start with the conventional nonmagnetic calculations performed in the local-density approximation (LDA). Using the Wannier function projection technique,¹⁷ one may obtain the values of the crystal-field splitting in the Ru t_{2g} subshell. Diagonalizing a small on-site t_{2g} - t_{2g} Hamiltonian, we found that the degeneracy of the Ru t_{2g} states is lifted due to a low symmetry (four out of six Ru-O bond lengths are different). The crystal-field splitting is 58 meV (between the lowest in energy and middle states) and 108 meV (between the middle and highest in energy orbitals). This is much smaller than the $2J_H \approx 1.4$ eV needed to stabilize the anti-Hund's rule state for the d^3 configuration with the total spin moment $S = 1/2$ per site.

However, a close inspection of the projected Hamiltonian shows that there are other terms even larger than the on-site splitting in the Ru t_{2g} shell. These are the hoppings between the Ru t_{2g} orbitals centered on different sites (exceeding 290 meV) and off-diagonal matrix elements between the Ru t_{2g} and Co e_g states (~ 100 meV). Thus, one may expect that the band structure in the vicinity of the Fermi level is rather governed by the intersite, not on-site, elements of the Hamiltonian, which is obviously a consequence of the dimerized crystal structure.

The LDA band structure is shown in Fig. 2. One may see that there are essentially three branches of the bands. Four bands placed exactly on the Fermi level mostly have the Co e_g character (see bottom panel in Fig. 2). Each band is two times degenerate in the ZT direction due to the fact that there are two formula units in the unit cell. The Co e_g bands are flat, which is related to the feature of the crystal structure: the CoO_6 octahedra are not directly connected to each other and are only connected via RuO_6 . Moreover, the Co-Ru-Co angle is close to 90° . The flat Co e_g bands provide an enormous density of states (DOS) at the Fermi level ~ 40 states/(eV f.u.), which results, as we will see below, in the magnetic instability according to the Stoner criteria.

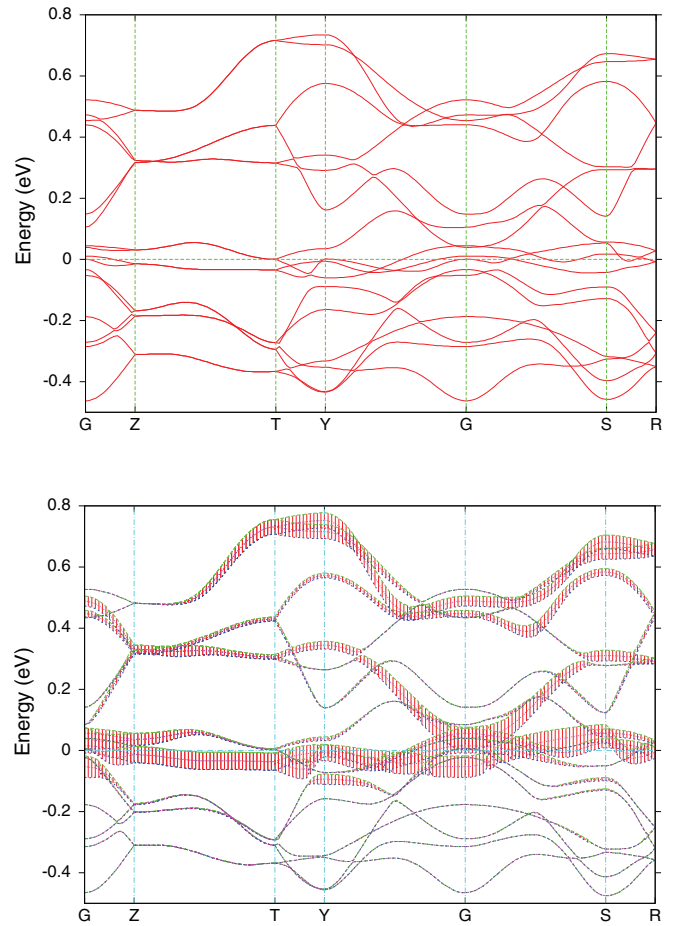


FIG. 2. (Color online) The band structure for $\text{Ba}_3\text{CoRu}_2\text{O}_9$, obtained in the LDA calculation. In the bottom panel the contribution coming from the Co e_g states is shown (so-called fat bands): the broader a given band is in a certain k point, the larger the contribution is from the Co e_g states. The local coordinate system with the axis pointing to oxygen ions was used to identify the Co e_g states. The Fermi level is set to zero.

The lowermost six bands, lying below the Co e_g bands, correspond to the Ru t_{2g} bonding states in the Ru-Ru dimer. The lowest, at ~ -0.3 eV in the ZT direction, are the a_{1g} orbitals, and the rest have e_g^π symmetry. Two a_{1g} orbitals of the neighboring Ru ions in the shared faces geometry are directed exactly toward each other. This leads to a large hopping between those wave functions, and as a result the bonding-antibonding splitting for the a_{1g} orbitals is much larger than for the e_g^π ones.

The uppermost six bands (spread from ~ 0.08 to 0.8 eV) are the Ru t_{2g} antibonding bands with an admixture of the Co e_g states.

IV. LSDA RESULTS

The large DOS at the Fermi level in the nonmagnetic LDA calculation leads to the magnetic instability. We used the LSDA as the simplest method to study magnetic properties of $\text{Ba}_3\text{CoRu}_2\text{O}_9$. This approach was shown to provide an adequate description of the Ru-based compounds.^{4,18} Experimentally determined magnetic structure⁶ was used in the

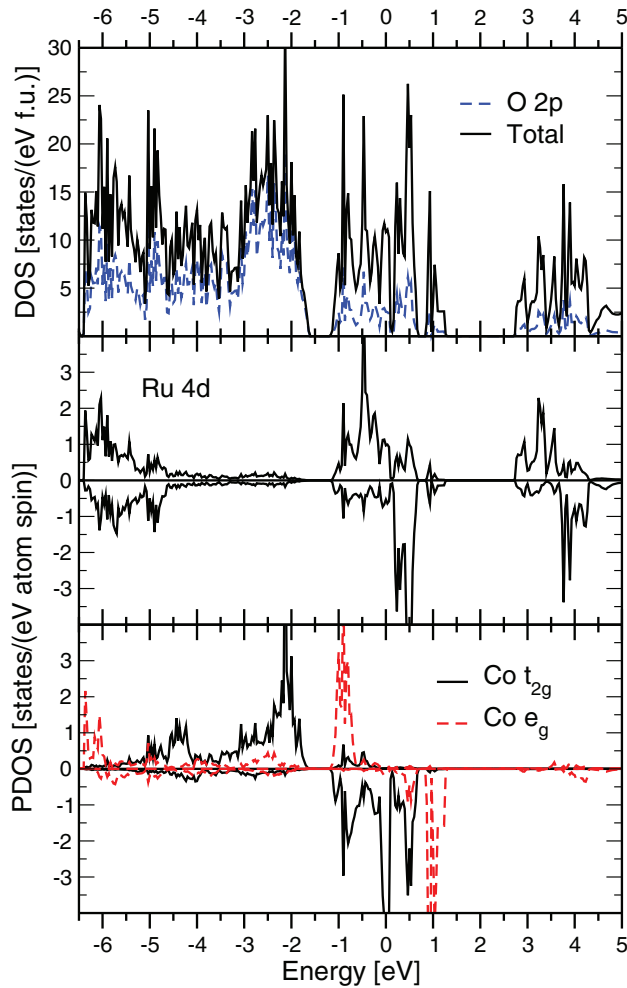


FIG. 3. (Color online) The total (TDOS) and partial (PDOS) density of states for Ba₃CoRu₂O₉, obtained in the LSDA calculation. The positive (negative) values on the lowest two plots correspond to spin majority (minority). The local coordinate system, when axes are directed to oxygen ions, was chosen to identify the Co t_{2g} and e_g states. The Fermi level is set to zero.

present calculations. It was shown that the Ru ions forming first magnetic lattice are paired antiferromagnetically in the dimers. The interdimer coupling in the c direction is also antiferromagnetic. The second magnetic lattice consists of the Co ions, which are antiferromagnetically paired in the c and b directions but ferromagnetically paired along the a direction (see Fig. 4 in Ref. 6).

The results of the LSDA calculation are presented in Fig. 3. The magnetic interaction splits the Co $3d$ states with different spins on ≈ 2 eV, which results in the formation of a sizable spin moment on the Co ion ($2.55\mu_B$). However, shifting the Co e_g states away from the Fermi level, the magnetic splitting puts the Co $t_{2g} \downarrow$ states in their place. As a result, in the LSDA Ba₃CoRu₂O₉ stays metallic, in contrast to the experimental observations.⁸ The magnetic moment on Ru ($1.1\mu_B$) is close to the experimentally measured value.^{6,7} In order to stabilize an insulating ground state in the following we will apply the LSDA + U method, which allows us to take into account strong on-site Coulomb correlations in a mean-field way.¹⁴

V. LSDA + U RESULTS

Since there are two transition-metal ions in Ba₃CoRu₂O₉, for which an account of the strong Coulomb correlations can be important, we applied the U correction step by step.

First of all, $U = 6$ eV and $J_H = 1$ eV were applied for the Co $3d$ shell only (denoted LSDA + U_{Co} in what follows). This results in the magnetic moments $|m_{Ru}| = 1.47\mu_B$, $|m_{Co}| = 2.61\mu_B$ and a band gap of 0.25 eV. This agrees both with experimental estimations of the magnetic moment on Ru of 1.17 – $1.45\mu_B$ ^{6,7} and semiconducting resistivity temperature dependence.⁸ It is important to note that the spin density is almost homogeneously distributed over all t_{2g} orbitals of the Ru⁵⁺ ion, leading to the orbital polarizations $|m_{t_{2g,1}}| = 0.49\mu_B$, $|m_{t_{2g,2}}| = 0.47\mu_B$, and $|m_{t_{2g,3}}| = 0.43\mu_B$ (the remaining $0.08\mu_B$ comes from the e_g orbitals). This is obviously due to the fact that the crystal-field splitting in the t_{2g} shell is significantly smaller than the intra-atomic Hund's rule exchange coupling J_H , as was shown in Sec. III.

The results obtained are stable with respect to the small variation of the U and J_H parameters. The decrease of J_H by 20% does not change either the spin moments or the band gap value. The calculation with $U = 5$ eV decreases the band gap by 0.01 eV and the spin moments by $0.01\mu_B$ and $0.04\mu_B$ for the Ru and Co atoms, respectively. Thus, the main effect of the U correction on the Co $3d$ states is to push them away from the Fermi level and stabilize the insulating ground state. This can be seen in Fig. 4.

In order to check that the solution obtained corresponds to the global minimum of the density functional in the LSDA + U approximation the fixed spin moment calculations were performed. One may see in Fig. 5 that the total energy of the system drastically grows with a decrease of the spin moment, making the state with $S = 1/2$ (low-spin state of Ru⁵⁺ ions), proposed in Ref. 8, energetically unfavorable. However, the minimum $E(\mu)$ by itself is flat enough, implying that the spin fluctuations may be operative in Ba₃CoRu₂O₉.

The intradimer exchange coupling was found to be antiferromagnetic, $J_{intra} = 211$ K, for the Heisenberg model as defined in Eq. (1) with $S = 3/2$. Each Ru-Ru dimer is connected with three other dimers on each side (i.e., with six dimers in a sum) via CoO₆ octahedra. The exchange coupling between the nearest Co and Ru ions (J_{Co}) is small and does not exceed 8 K. The coupling between dimers is larger, $J_{inter} = 30.4$, 30.4, and 16.6 K. So in the LSDA + U_{Co} method Ba₃CoRu₂O₉ should be considered to be a system of coupled dimers.

In the second step we added the U correction for the Ru $4d$ states with $U = 3$ eV and $J_H = 0.7$ eV, so that both Ru $4d$ and Co $3d$ states were considered to be correlated (abbreviated LSDA + $U_{Co,Ru}$). As a result, both the magnetic moment on Ru and the band gap grew in absolute value. The spin moments were found to be $|m_{Ru}| = 1.95\mu_B$, $|m_{Co}| = 2.61\mu_B$, while the band gap equals 1.11 eV. The exchange constants are as follows: $J_{intra} = 150$ K, $J_{inter,1} = 39.8$ K, $J_{inter,2} = 39.8$ K, $J_{inter,3} = 19.4$ K.

Comparing calculated and experimental values of the local magnetic moments, one may see that while the LSDA + U method significantly improves the calculation results when the U correction is applied only to the Co $3d$ states, it makes

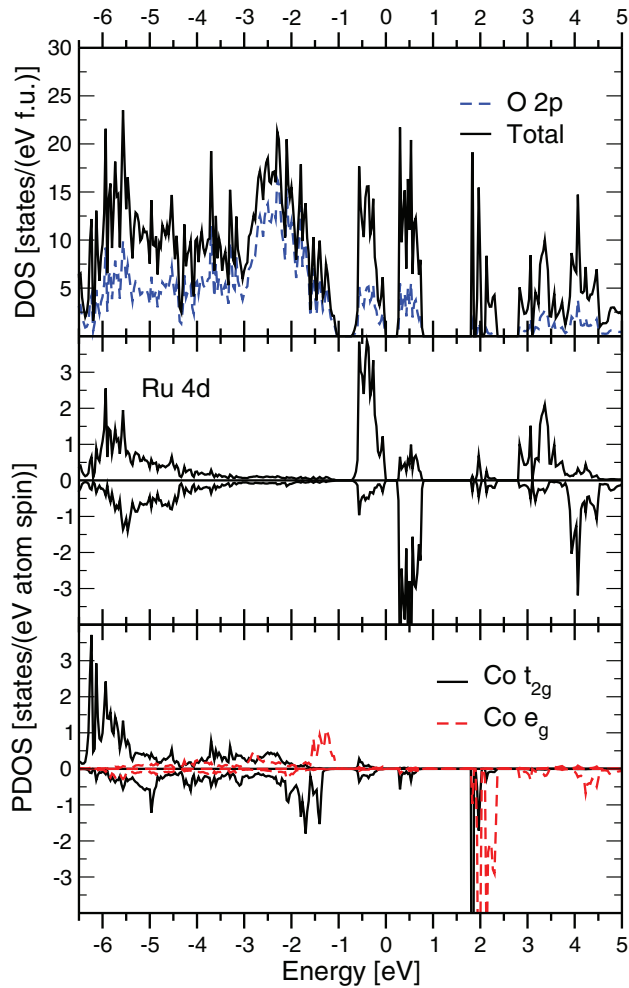


FIG. 4. (Color online) The total (TDOS) and partial (PDOS) density of states for $\text{Ba}_3\text{CoRu}_2\text{O}_9$, obtained in the $\text{LSDA} + U_{\text{Co}}$ calculation. The positive (negative) values on the lowest two plots correspond to spin majority (minority). The local coordinate system, when axes are directed toward oxygen ions, was chosen to identify the $\text{Co } t_{2g}$ and e_g states. The Fermi level is set to zero.

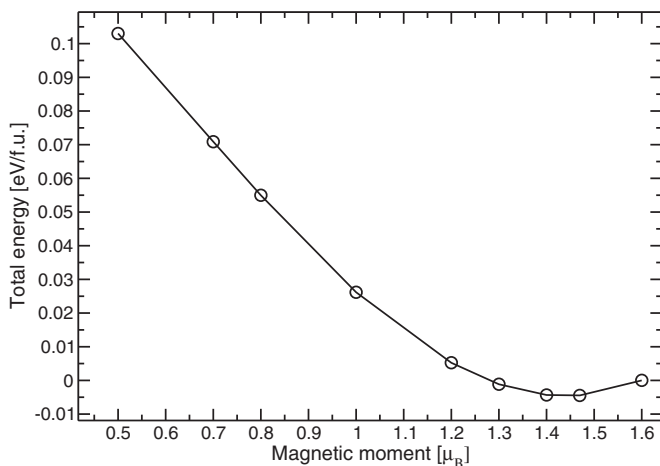


FIG. 5. The total energy dependence on the spin moment, obtained in the fixed spin moment calculations in the $\text{LSDA} + U_{\text{Co}}$ approximation.

agreement with experiment worse if it is used for both the Ru $4d$ and Co $3d$ states.

The $\text{LSDA} + U$ method was designed to describe electronic and magnetic properties of the $3d$ transition-metal compounds. In the traditional realization of this method for the description of the electronic properties of the transition-metal oxides the U correction is applied only to the d wave functions:

$$H_{\text{LSDA}+U} = H_{\text{LSDA}} + \sum_{mm'} |\psi_{inlm\sigma}\rangle V_{mm'}^\sigma \langle \psi_{inlm'\sigma}|. \quad (2)$$

Here i is the site index, n, l, m are the principal, orbital, and magnetic quantum numbers, respectively, H_{LSDA} is the LSDA Hamiltonian, and $V_{mm'}^\sigma$ is the U correction as defined in Ref. 14. In the LMTO method $\psi_{inlm\sigma}$ are the corresponding linearized muffin-tin (LMT) orbitals^{12,19} for d states, and in the linearized augmented plane wave (LAPW) method, they are the “muffin-tin” part of a radial function for the d orbital.²⁰

However, in the compounds based on the $4d$ and $5d$ transition-metal ions or even $3d$ ions with a high oxidation state the electrons of interest are localized on the orbitals which significantly differ from the atomic d wave functions (see, e.g., Fig. 6 in Ref. 21, where the orbital on which one of the Au $5d$ electrons localizes in $\text{Cs}_2\text{Au}_2\text{Cl}_6$ is shown). An application of the Hubbard-like U correction only to the d part of the wave function is methodologically incorrect. The use of Wannier functions centered on the transition-metal ions, but with large contributions to the surrounding atoms, is more appropriate in this case. The corresponding version of the $\text{LDA} + U$ method in the Wannier function basis set was recently proposed.²²

The squared coefficients of the Wannier function expansion in terms of the LMT orbitals show the contribution of each orbital.²³ In the case of $\text{Ba}_3\text{CoRu}_2\text{O}_9$ the Wannier functions, centered on the Ru ions and corresponding to the LDA bands expanded from -0.5 to 0.8 eV, have a contribution from the Ru $4d$ LMT orbitals of only 55%, while $\sim 40\%$ corresponds to the O $2p$ orbitals and $\sim 5\%$ corresponds to the Co $3d$ orbitals. Thus, applying the U correction on the Ru $4d$ states, we act only on part of the wave function and force the electrons to localize on the atomic d orbitals, not on the Wannier functions preferred by the LDA. This results in the overestimation of the spin moment on Ru and the band gap in the $\text{LSDA} + U_{\text{Co,Ru}}$ calculations. A nonphysical increase of the U parameter on Ru up to 12 eV leads to the Ru spin moment of $2.74\mu_B$, which is close to what one would expect for the d^3 configuration if electrons localize on the atomic d orbitals.

Thus, we see that a small value of the spin moment on Ru ($1.47\mu_B$) in the $\text{LSDA} + U_{\text{Co}}$ calculation is related to the fact that the electrons are indeed localized on the Wannier functions, which have a substantial contribution from the O $2p$ states. A naive estimation of the Ru spin moment from the Ru $4d$ contribution to the LDA Wannier functions ($3 \times 0.55 = 1.65$) is close to what we obtain in the real $\text{LSDA} + U_{\text{Co}}$ calculation.

An alternative mechanism of the magnetic moment reduction on Ru is a stabilization of the “orbital-selective spin-singlet” state. The large bonding-antibonding splitting may lead to the formation of the spin singlets on the a_{1g} orbitals, while the electrons occupying the e_g^π orbitals may stay localized and bear magnetic moment ($2\mu_B$), which can be again reduced by the hybridization with oxygen. The

intra-atomic Hund's rule exchange will act against this state, but a final answer should be given by a direct calculation. The one-electron approximations, such as LSDA and LSDA + U , are useless in this situation since they are not able to simulate the spin-singlet state, which should be described by a true many-particle wave function. The cluster dynamical mean-field theory should be used instead.

VI. CONCLUSIONS

With the use of the LSDA + U calculations (with the U correction applied to the Co 3d states) we show that the electronic ground state in the low-temperature phase of Ba₃CoRu₂O₉ follows the Hund's rule with a $(t_{2g}\uparrow)^3$ electronic configuration (all Ru d electrons on one site have the same spin). This is in contrast to the unusual orbital filling $(t_{2g}\uparrow)^2(t_{2g}\downarrow)^1$ proposed previously based on the crystal structure analysis.⁸ A very similar situation was observed in the case of La₄Ru₂O₁₀, where the stabilization of the low-spin state of the Ru⁴⁺ was first proposed experimentally.²⁴ However, band structure calculations together with x-ray measurements showed that this is unlikely.³ In Ba₃CoRu₂O₉ the suppression of the

magnetic moment on the Ru ions from the $3\mu_B$ expected from the naive atomic consideration to the $1.17\text{--}1.45\mu_B$ observed in the experiment^{6,7} is attributed to the strong hybridization effects. Due to the large spatial expansion of the 4d wave functions and the high oxidation state of Ru (5+) the Ru 4d and O 2p states are strongly hybridized. As a result, three d electrons of Ru⁵⁺ localize not on the atomic but on the Wannier orbitals, with significant contributions from the spin nonpolarized O 2p states. We also show that the LSDA + U approximation must be applied with care for the description of the 4d and 5d transition-metal compounds.

ACKNOWLEDGMENTS

I am grateful to Professor D. Khomskii for the various discussions about the suppression of the magnetic moment in the dimer and trimer systems. The calculations were performed on the "Uran" cluster. This work is supported by the Russian Foundation for Basic Research via Grant No. RFFI-13-02-00374 and by the Ministry of Education and Science of Russia through programs 12.740.11.0026 and MK-3443.2013.2.

*streltsov@imp.uran.ru

- ¹I. I. Mazin, H. O. Jeschke, K. Foyevtsova, R. Valentí, and D. I. Khomskii, *Phys. Rev. Lett.* **109**, 197201 (2012).
- ²S. A. J. Kimber, M. S. Senn, S. Fratini, H. Wu, A. H. Hill, P. Manuel, J. P. Attfield, D. N. Argyriou, and P. F. Henry, *Phys. Rev. Lett.* **108**, 217205 (2012).
- ³H. Wu, Z. Hu, T. Burnus, J. Denlinger, P. Khalifah, D. Mandrus, L.-Y. Jang, H. Hsieh, A. Tanaka, K. Liang *et al.*, *Phys. Rev. Lett.* **96**, 256402 (2006).
- ⁴S. V. Streltsov and D. I. Khomskii, *Phys. Rev. B* **86**, 064429 (2012).
- ⁵A. S. Erickson, S. Misra, G. J. Miller, R. R. Gupta, Z. Schlesinger, W. A. Harrison, J. M. Kim, and I. R. Fisher, *Phys. Rev. Lett.* **99**, 016404 (2007).
- ⁶P. Lightfoot and P. D. Battle, *J. Solid State Chem.* **89**, 174 (1990).
- ⁷J. T. Rijssenbeek, Q. Huang, R. W. Erwin, H. W. Zandbergen, and R. J. Cava, *J. Solid State Chem.* **146**, 65 (1999).
- ⁸H. D. Zhou, A. Kiswandhi, Y. Barlas, J. S. Brooks, T. Siegrist, G. Li, L. Balicas, J. G. Cheng, and F. Rivadulla, *Phys. Rev. B* **85**, 041201(R) (2012).
- ⁹J. T. Rijssenbeek, P. Matl, B. Batlogg, N. P. Ong, and R. J. Cava, *Phys. Rev. B* **58**, 10315 (1998).
- ¹⁰S. Lee, J.-G. Park, D. Adroja, D. Khomskii, S. Streltsov, K. A. McEwen, H. Sakai, K. Yoshimura, V. I. Anisimov, D. Mori *et al.*, *Nat. Mater.* **5**, 471 (2006).
- ¹¹K. Momma and F. Izumi, *J. Appl. Crystallogr.* **44**, 1272 (2011).
- ¹²O. K. Andersen and O. Jepsen, *Phys. Rev. Lett.* **53**, 2571 (1984).

- ¹³U. von Barth and L. Hedin, *J. Phys. C* **5**, 1629 (1972).
- ¹⁴V. Anisimov, F. Aryasetiawan, and A. Lichtenstein, *J. Phys.: Condens. Matter* **9**, 767 (1997).
- ¹⁵A. Dyachenko, A. Shorikov, A. Lukoyanov, and V. Anisimov, *JETP Lett.* **96**, 56 (2012).
- ¹⁶A. Liechtenstein, V. Gubanov, M. Katsnelson, and V. Anisimov, *J. Magn. Magn. Mater.* **36**, 125 (1983).
- ¹⁷S. V. Streltsov, A. S. Mylnikova, A. O. Shorikov, Z. V. Pchelkina, D. I. Khomskii, and V. I. Anisimov, *Phys. Rev. B* **71**, 245114 (2005).
- ¹⁸C. Etz, I. V. Maznichenko, D. Böttcher, J. Henk, A. N. Yaresko, W. Hergert, I. I. Mazin, I. Mertig, and A. Ernst, *Phys. Rev. B* **86**, 064441 (2012).
- ¹⁹V. I. Anisimov, J. Zaanen, and O. K. Andersen, *Phys. Rev. B* **44**, 943 (1991).
- ²⁰A. B. Shick, A. I. Liechtenstein, and W. E. Pickett, *Phys. Rev. B* **60**, 10763 (1999).
- ²¹A. Ushakov, S. V. Streltsov, and D. I. Khomskii, *J. Phys.: Condens. Matter* **23**, 445601 (2011).
- ²²D. Korotin, V. Kukolev, A. V. Kozhevnikov, D. Novoselov, and V. I. Anisimov, *J. Phys.: Condens. Matter* **24**, 415603 (2012).
- ²³V. Anisimov, D. Kondakov, A. Kozhevnikov, I. Nekrasov, Z. Pchelkina, J. Allen, S.-K. Mo, H.-D. Kim, P. Metcalfe, S. Suga *et al.*, *Phys. Rev. B* **71**, 125119 (2005).
- ²⁴P. Khalifah, R. Osborn, Q. Huang, H. W. Zandbergen, R. Jin, Y. Liu, D. Mandrus, and R. J. Cava, *Science* **297**, 2237 (2002).